Supporting Information for

Divergent Trends of Black and Brown Carbon Driven by Anthropogenic Emissions and Open Biomass Burning Across Asia

Ying Zhang[1,2,3], Abudurexiati Abulimiti[3], Yan-Lin Zhang[3*]

[1]State Key Laboratory of Climate System Prediction and Risk Management/Key Laboratory of Meteorological Disaster, Ministry of Education/Collaborative Innovation Center on Forecast and Evaluation of Meteorological Disasters, Nanjing University of Information Science and Technology, Nanjing 210044, China

[2]School of Atmospheric Sciences, Nanjing University of Information Science and Technology, Nanjing 210044, Chian

[3]School of Ecology and Applied Meteorology, Nanjing University of Information Science and Technology. Nanjing 210044, China

[*]Corresponding author: Yan-Lin Zhang (zhangyanlin@nuist.edu.cn or dryanlinzhang@outlook.com)

Contents of this file

Text S1: Emissions of primary brown carbon

Emissions of primary brown carbon (BRpri) were obtained from organic carbon (OC) inventories using the mass ratio M_{BRpri}/M_{OC}, as noted in the main text (Section 2.1.2).

Following Jo et al. (2016), the ratio M_{BRpri}/M_{OC} is determined using emission factors (EF) of BC and OC, mass absorption efficiencies (MAE) of BC (7.5 $m^2\ g^{-1}$) and BRpri (1.0 $m^2\ g^{-1}$), and the absorption coefficient ratio $B_{abs,BRpri}/B_{abs,BC}$, expressed as

$$\frac{M_{BRpri}}{M_{OC}} = \frac{B_{abs,BRpri}}{B_{abs,BC}} \times \frac{MAE_{BC}}{MAE_{BRpri}} \times \frac{EF_{BC}}{EF_{OC}} \quad (S1)$$

By assuming BC and BRpri are the only two light-absorbing species of combustion-emitted carbonaceous aerosols (CAs), the absorption coefficient ratio $B_{abs,BRpri}/B_{abs,BC}$ can be derived from

$$\left(1 + \frac{B_{abs,BRpri}}{B_{abs,BC}}\right)\left(\frac{\lambda}{\lambda_0}\right)^{-AAE_{CAs}} = \left(\frac{B_{abs,BRpri}}{B_{abs,BC}}\right)\left(\frac{\lambda}{\lambda_0}\right)^{-AAE_{BRpri}} + \left(\frac{\lambda}{\lambda_0}\right)^{-AAE_{BC}} \quad (S2)$$

where λ0 is 550 nm and λ is set as wavelengths from 300 to 900 nm with the interval of 50 nm for the regression. The absorption Angstrom exponents (AAE) of BC (1.0) and BRpri (5.48) are adopted from Jo et al. (2016); AAE_{CAs} is calculated as,

$$AAE_{CAs} = -17.34 \times MCE + 18.20 \quad (S3)$$

where MCE is the modified combustion efficiency, calculated by the molecular weights and EFs of CO_2 and CO (Eq. S4).

$$MCE = \frac{\Delta CO2}{\Delta CO2 + \Delta CO} = \frac{EF_{CO2}/MW_{CO2}}{EF_{CO2}/MW_{CO2} + EF_{CO}/MW_{CO}} \quad (S4)$$

Emissions of BRpri from both open biomass burning (OBB) and residential solid fuel combustion (RES) were estimated using this method. The corresponding OC inventories and parameters used in the calculations (i.e., EF_{BC}, EF_{OC}, EF_{CO2}, EF_{CO}, MCE) are summarized in Table S1.

Text S2: Observation-derived absorption of BrC in Nanjing

Ambient aerosols were collected through a $PM_{2.5}$ inlet at Nanjing University of Information Science and Technology (NUIST, 38.21°N, 118.72°E) from January to December 2019. Their light absorption coefficients at seven wavelengths (370, 470, 520, 590, 660, 880, 950 nm) were measured using an Aethalometer (AE33, Magee Scientific, USA) at a flow rate of 5 L min^{-1}. Detailed information on the instrument and its measurement principle can be found in Drinovec et al. (2015). Filter-based absorption measurements are affected by both the loading effect and filter matrix scattering effect (Coen et al., 2010). In the AE33, the loading effect is compensated for using the dual-spot measurement technique, while a multiple scattering correction factor of 1.39 was applied as the default value for the M8060 filter tape (Savadkoohi et al., 2023).

Atmospheric aerosol light absorption is mainly attributed to BC, BrC and mineral dust. In this study, mineral dust was assumed to have a negligible influence since the AE33 was operated with a $PM_{2.5}$ impactor and dust storm influence at the sampling site was limited. Thus, as indicated by previous studies (Bao et al., 2021; Chow et al., 2018; Meda et al., 2025), the total light absorption at a certain wavelength can be expressed as,

$$B_{abs}(\lambda) = B_{abs,BC}(\lambda) + B_{abs,BrC}(\lambda) \tag{S5}$$

Then, a simplified two component model was used to estimate the contribution of BC and BrC at a certain wavelength as follows,

$$B_{abs}(\lambda) = q_{BC} \times \lambda^{-AAE_{BC}} + q_{BrC} \times \lambda^{-AAE_{BrC}} \tag{S6}$$

where q_{BC} and q_{BrC} are fitting coefficients, and AAE_{BC} and AAE_{BrC} are the absorption Ångström exponent of BC and BrC, respectively. Here, AAE_{BC} assumed to be 1, Eq. (S6) can be simplified as,

$$\lambda \times B_{abs}(\lambda) = q_{BC} + q_{BrC} \times \lambda^{(1-AAE_{BrC})} \tag{S7}$$

For each potential AAE_{BrC} value between 1.5 to 15, the fitting coefficients were determined by least-squares minimization between the calculated and measured values. The AAE_{BrC} corresponding to the lowest mean squared error (MSE) was selected as the effective AAE_{BrC}. Previous study noted that the AAE of internally mixed BC can vary from 0.55 to 1.7, and assuming AAE_{BC} of 1 may introduce an uncertainty of up to 20% (Zotter et al., 2017).

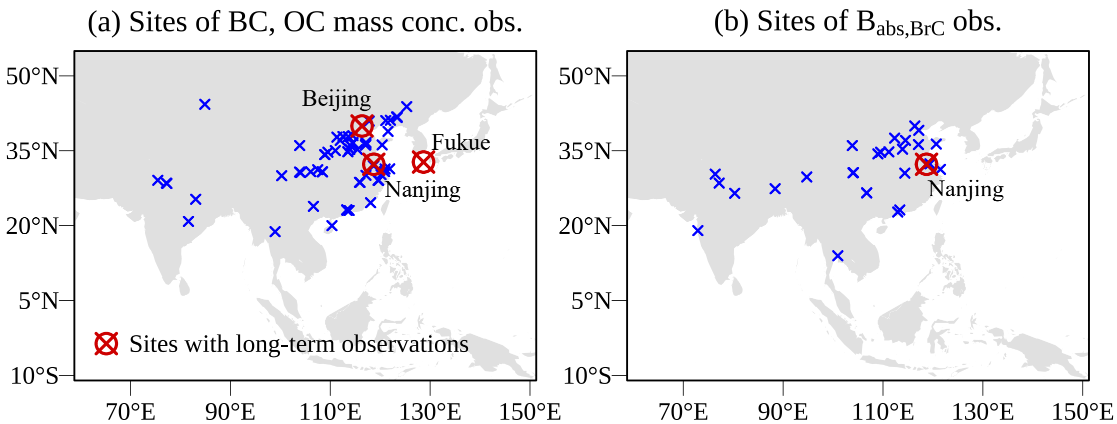

Figure S1. Study area and observation sites for (a) BC and OC mass concentrations and (b) BrC absorption ($B_{abs,BrC}$).

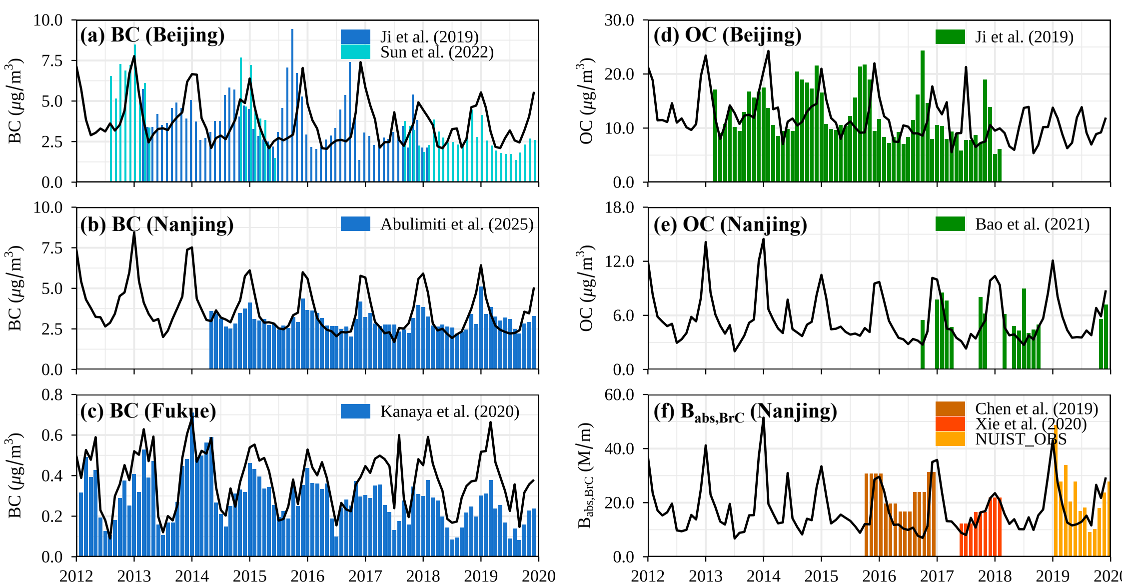

Figure S2. Comparison between simulation (black line) and observation (colored bar): (a-c) BC and (d-e) OC mass concentrations, (f) BrC absorption ($B_{abs,BrC}$) at 370 nm.

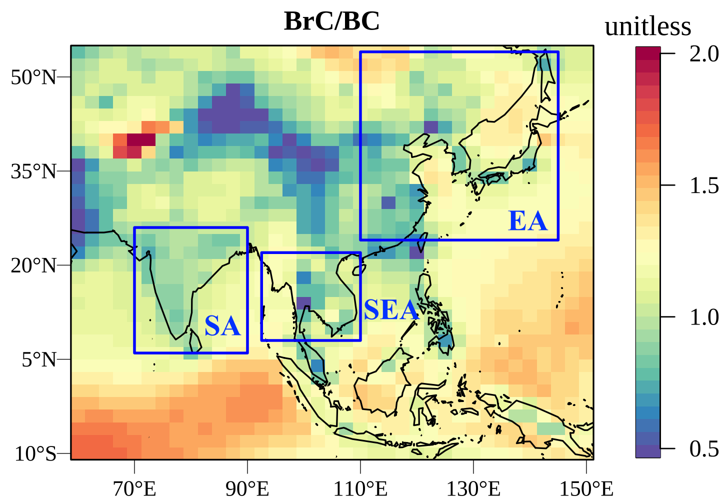

Figure S3. Multi-year (2012–2019) mean BrC/BC over Asia. East Asia (EA), South Asia (SA) and Southeast Asia (SEA) are highlighted with blue rectangles.

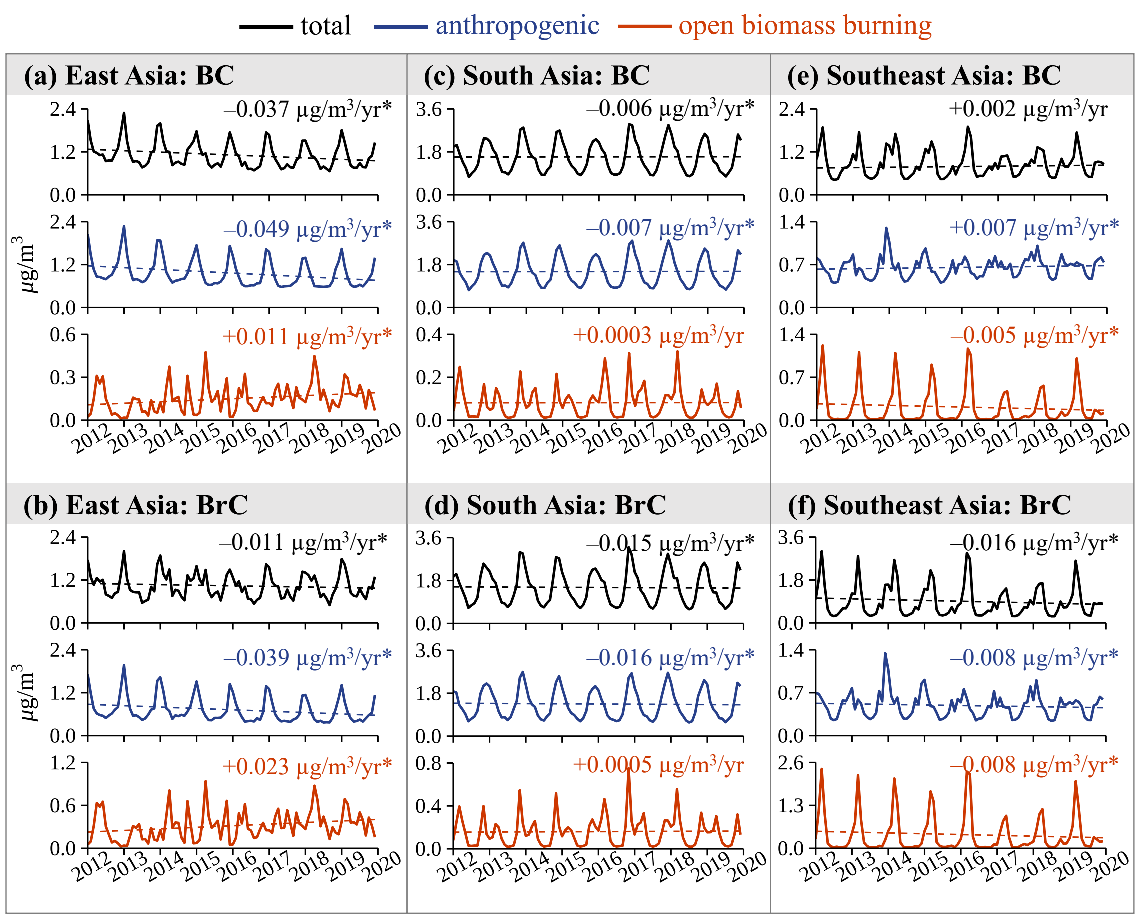

Figure S4. Time series of BC and BrC in East Asia, South Asia and Southeast Asia. Trends (dash line) with slope and statistical significance ($p < 0.05$, denoted by *) are shown inset.

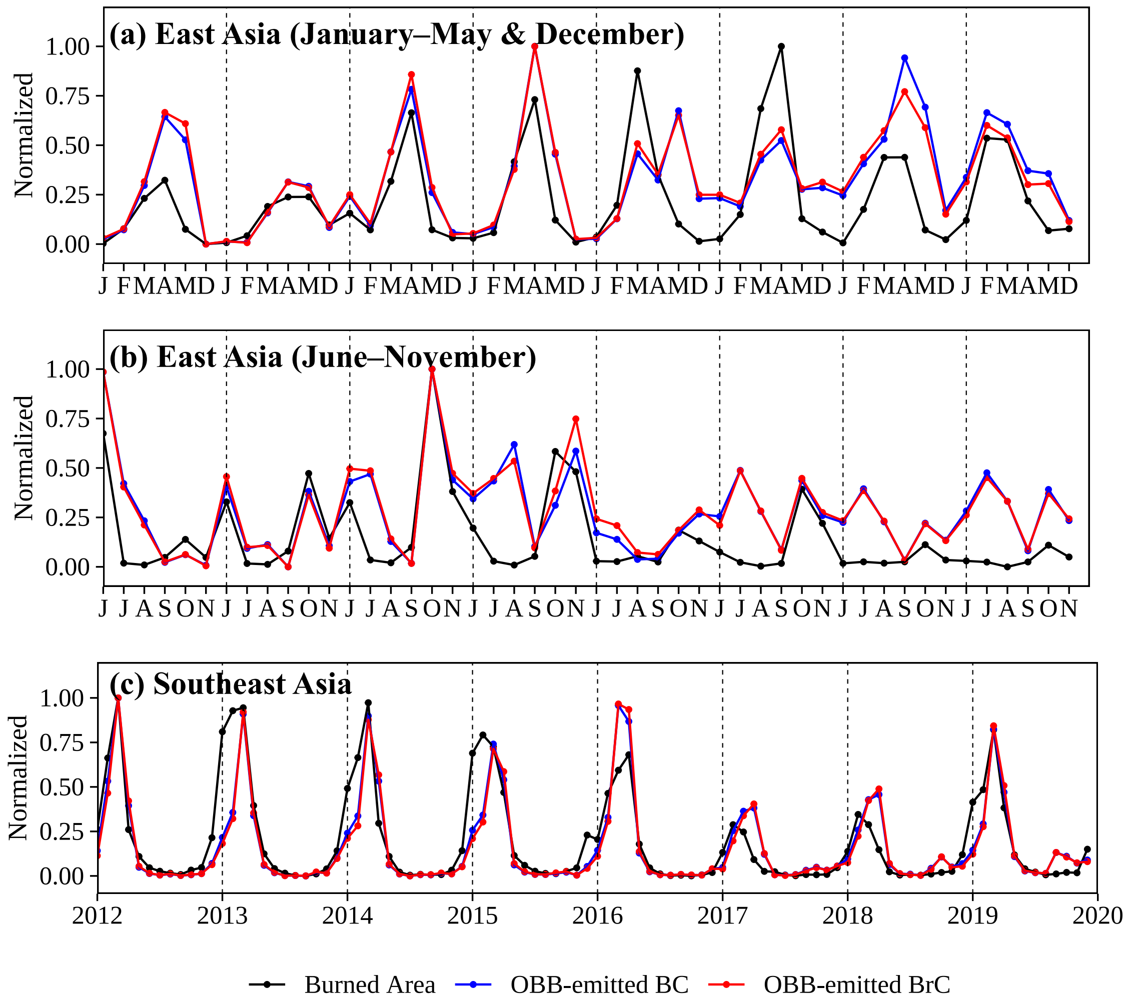

Figure S5. Simulations of OBB-emitted BC and BrC concentrations (normalized) compared to satellite-retrieved burned area (normalized): (a–b) East Asia and (c) Southeast Asia.

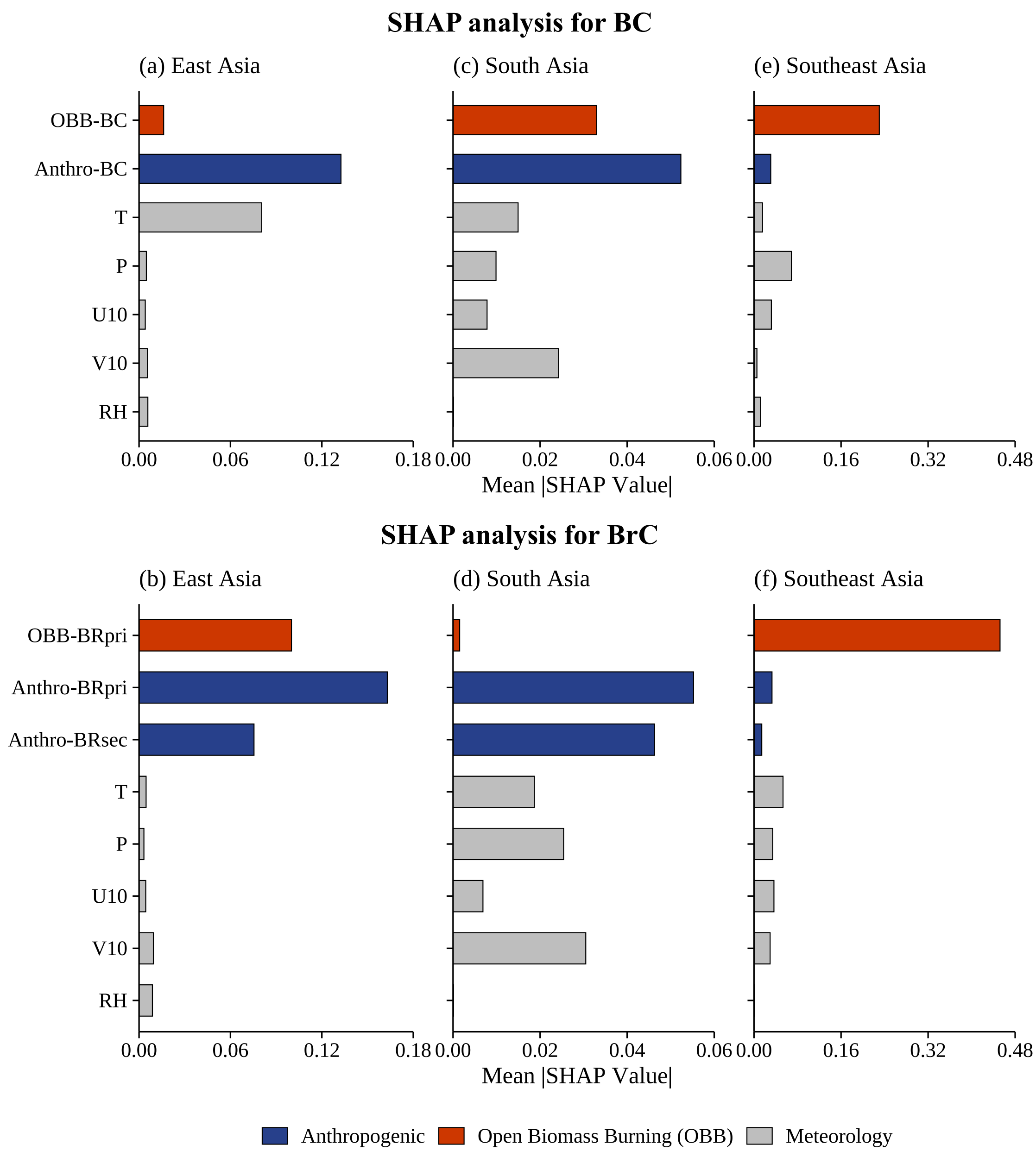

Figure S6. Relative importance of emissions (anthropogenic and OBB) and meteorological variables (T: temperature; P: pressure; U10: 10 m zonal wind; V10: 10 m meridional wind; RH: relative humidity) for long-term variations of (a-c) BC and (d-f) BrC.

Table S1. OC inventories and parameters used for BRpri emission calculations.

Source	Inventory	EF_{BC} (g/kg)	EF_{OC} (g/kg)	EF_{CO2} (g/kg)	EF_{CO} (g/kg)	Modified Combustion Efficiency (MCE)
OBB[a]	FEER	$\frac{ER_{BC}}{ER_{PM2.5}}$	$\frac{ER_{OC}}{ER_{PM2.5}}$	$\frac{ER_{CO2}}{ER_{PM2.5}}$	$\frac{ER_{CO}}{ER_{PM2.5}}$	Calculated by Eq. (S4)
RES[b]	CEDS	0.52	2.39	/	/	0.925

[a]Emissions from open biomass burning (OBB). Emission factor (EF) of species are calculated using the emission rate (ER) provided by FEER.

[b]Emissions from residential solid fuel combustion (RES). EFs of BC and OC are obtained from https://github.com/emcduffie/CEDS/tree/CEDS_GBD -MAPS. Due to the lack of EF_{CO2} and EF_{CO}, the MCE measured for wood, crop and coal combustion (Chen et al., 2012; Qian et al., 2021; Stockwell et al., 2014) is used instead.

Table S2. Estimated emissions of BRpri from open biomass burning (OBB) and residential solid fuel combustion (RES), compared to a bottom-up inventory (Xiong et al., 2022).

	Global Emission of BRpri			Mass Ratio M_{BRpri}/M_{OC}		
	Total	OBB	RES	Total	OBB	RES
this study	8.58 Tg C/yr	63%	37%	20.5%	19%	26%
(Xiong et al., 2022)	7.26 Tg C/yr	57%	43%	20%	16%±2%	29%±2%

Table S3. Imaginary refractive index (*k*) of BRpri and BRsec used in this study.

Species	300 nm	400 nm	440 nm	550 nm	550 nm
BRpri (k_{BRpri})	0.291	0.120	0.078	0.047	0.034
BRsec (k_{BRsec})	0.036	0.007	0.006	0.006	0.006

Table S4. Short-term site observations of BC and OC mass concentrations collected from previous studies.

Table S5. Short-term site observations of BrC absorption collected from previous studies.

Table S6. Optimized hyperparameters and performance metrics of RF statistical models built separately for East, South and Southeast Asia (EA, SA, SEA).

Regions	Hyperparameters			10-fold cross validation	test set validation
	n_estimators	max_depth	min_sample_leaf	R^2	R^2
analysis for BC					
EA	100	6	4	0.70	0.73
SA	107	15	4	0.61	0.65
SEA	100	10	4	0.82	0.82
analysis for BrC					
EA	90	6	4	0.61	0.63
SA	111	6	4	0.58	0.65
SEA	100	10	4	0.88	0.88
analysis for BrC/BC					
EA	100	15	4	0.76	0.78
SA	100	15	4	0.67	0.72
SEA	100	15	4	0.94	0.94

Table S7. Estimated clear-sky DRF of BC and BrC from this study (averaged over 2012–2019) compared with previous studies.

Regions	DRF (W m^{-2})	this study	previous studies	
East Asia	BC	0.92	1.06 (all sky)	(X. Zhang et al., 2020)
			0.91~1.23	(Yang et al., 2024)
	BrC	0.35	0.40	(Zhou et al., 2025)
			0.11~0.15	(Yang et al., 2024)
			0.11~0.21	(Xu et al., 2024)
South Asia	BC	1.69	1.2~4	(A. Zhang et al., 2020)
	BrC	0.86	0.3~0.6	(A. Zhang et al., 2020)
			0.3~0.8	(Xie et al., 2025)
			0.5~2	(Navinya et al., 2025)
Southeast Asia	BC	0.81	0.4~2	(A. Zhang et al., 2020)
			2.70	(Huang et al., 2025)
	BrC	0.58	0.3~0.6	(A. Zhang et al., 2020)
			0.3~0.6	(Xie et al., 2025)
			0.58	(Huang et al., 2025)

Reference

Bao, M., Zhang, Y.-L., Cao, F., Lin, Y.-C., Wang, Y., Liu, X., et al. (2021). Highly time-resolved characterization of carbonaceous aerosols using a two-wavelength Sunset thermal–optical carbon analyzer. *Atmospheric Measurement Techniques*, *14*(6), 4053–4068.

Chen, Y., Roden, C. A., & Bond, T. C. (2012). Characterizing biofuel combustion with patterns of real-time emission data (PaRTED). *Environmental Science & Technology*, *46*(11), 6110–6117.

Chow, J. C., Watson, J. G., Green, M. C., Wang, X., Chen, L.-W. A., Trimble, D. L., et al. (2018). Separation of brown carbon from black carbon for IMPROVE and Chemical Speciation Network PM2. 5 samples. *Journal of the Air & Waste Management Association*, *68*(5), 494–510.

Coen, C. M., Weingartner, E., Apituley, A., Ceburnis, D., Fierz-Schmidhauser, R., Flentje, H., et al. (2010). Minimizing light absorption measurement artifacts of the Aethalometer: evaluation of five correction algorithms. *Atmospheric Measurement Techniques*, *3*(2), 457–474.

Drinovec, L., Močnik, G., Zotter, P., Prévôt, A., Ruckstuhl, C., Coz, E., et al. (2015). The "dual-spot" Aethalometer: an improved measurement of aerosol black carbon with real-time loading compensation. *Atmospheric Measurement Techniques*, *8*(5), 1965–1979.

Huang, Y., Lu, X., Li, Z., Fung, J. C. H., Wang, Y., & Chen, Y. (2025). Direct radiative effects of black carbon and brown carbon from Southeast Asia biomass burning with the WRF-CMAQ two-way coupled model. *Environmental Pollution*, *366*, 125425. https://doi.org/10.1016/j.envpol.2024.125425

Jo, D. S., Park, R. J., Lee, S., Kim, S.-W., & Zhang, X. (2016). A global simulation of brown carbon: implications for photochemistry and direct radiative effect. *Atmospheric Chemistry and Physics*, *16*(5), 3413–3432. https://doi.org/10.5194/acp-16-3413-2016

Meda, B. N. M., Sarangi, C., Ali, S., M, V., Nair, V. S., Kumar, A., et al. (2025). Spatiotemporal Variability and Radiative Forcing of Secondary Brown Carbon over India. *ACS ES&T Air*, *2*(11), 2376–2387.

Navinya, C., Kapoor, T. S., Venkataraman, C., Phuleria, H. C., & Chakrabarty, R. K. (2025). Brown carbon light absorption over India: Research status and need for discerning climate impacts. *ACS Es&t Air*, *2*(7), 1115–1135.

Qian, Z., Chen, Y., Liu, Z., Han, Y., Zhang, Y., Feng, Y., et al. (2021). Intermediate volatile organic compound emissions from residential solid fuel combustion based on field measurements in rural China. *Environmental Science & Technology*, *55*(9), 5689–5700.

Savadkoohi, M., Pandolfi, M., Reche, C., Niemi, J. V., Mooibroek, D., Titos, G., et al. (2023). The variability of mass concentrations and source apportionment analysis of equivalent black carbon across urban Europe. *Environment International*, *178*, 108081.

Stockwell, C., Yokelson, R., Kreidenweis, S., Robinson, A., DeMott, P., Sullivan, R., et al. (2014). Trace gas emissions from combustion of peat, crop residue, domestic biofuels, grasses, and other fuels: configuration and Fourier transform infrared (FTIR) component of the fourth Fire Lab at Missoula Experiment (FLAME-4). *Atmospheric Chemistry and Physics*, *14*(18), 9727–9754.

Xie, X., Zhang, Y., Liang, R., & Wang, X. (2025). Global modeling of brown carbon: impact of temperature- and humidity-dependent bleaching. *Atmospheric Chemistry and Physics*, *25*(20), 13547–13561. https://doi.org/10.5194/acp-25-13547-2025

Xiong, R., Li, J., Zhang, Y., Zhang, L., Jiang, K., Zheng, H., et al. (2022). Global brown carbon emissions from combustion sources. *Environmental Science and Ecotechnology*, *12*, 100201. https://doi.org/10.1016/j.ese.2022.100201

Xu, L., Lin, G., Liu, X., Wu, C., Wu, Y., & Lou, S. (2024). Constraining Light Absorption of Brown Carbon in China and Implications for Aerosol Direct Radiative Effect. *Geophysical Research Letters*, *51*(16), e2024GL109861. https://doi.org/10.1029/2024GL109861

Yang, L., Mao, Y., Liao, H., Xie, M., & Zhang, Y. (2024). Direct radiative forcing of light-absorbing carbonaceous aerosols in China. *Atmospheric Research*, *304*, 107396.

Zhang, A., Wang, Y., Zhang, Y., Weber, R. J., Song, Y., Ke, Z., & Zou, Y. (2020). Modeling the global radiative effect of brown carbon: a potentially larger heating source in the tropical free troposphere than black carbon. *Atmospheric Chemistry and Physics*, *20*(4), 1901–1920. https://doi.org/10.5194/acp-20-1901-2020

Zhang, X., Chen, S., Kang, L., Yuan, T., Luo, Y., Alam, K., et al. (2020). Direct radiative forcing induced by light-absorbing aerosols in different climate regions over East Asia. *Journal of Geophysical Research: Atmospheres*, *125*(14), e2019JD032228.

Zhou, J., Wu, J., Su, X., Wang, R., El Haddad, I., Li, X., et al. (2025). Source-explicit estimation of brown carbon in the polluted atmosphere over the North China Plain: implications for distribution, absorption, and the direct radiative effect. *Atmospheric Chemistry and Physics*, *25*(14), 7563–7580.

Zotter, P., Herich, H., Gysel, M., El-Haddad, I., Zhang, Y., Močnik, G., et al. (2017). Evaluation of the absorption Ångström exponents for traffic and wood burning in the Aethalometer-based source apportionment using radiocarbon measurements of ambient aerosol. *Atmospheric Chemistry and Physics*, *17*(6), 4229–4249.